Coherent Radiation Diagnostics of Parameters of Nanostructures at Electron Accelerators

V. K. Grishin[a], B. S. Ishkhanov[a], V. I. Shvedunov[a], and N. N. Nasonov[b]

[a] *Skobeltsyn Institute of Nuclear Physics, Moscow State University, Leninskie gory, Moscow, 119992 Russia*
e-mail: grishin@depni.npi.msu.ru

[b] *Belgorod State University, ul. Studentcheskaja 14, Belgorod, 308007 Russia*

Abstract—The possibility of observing and diagnosing parameters of nanoobjects in a substance by using coherent X-ray radiation arising from the direct interaction of accelerated electrons with the object of interest is discussed. It is analytically shown that analysis of the generated radiation allows the microstructural features of the nanoobject to be studied. To illustrate the main conclusions, coherent radiation generated by relativistic electron scattering on fullerene is considered.

1. The most important condition for the use of nanotechnologies is reliable diagnosis of the parameters of nanostructures. Hard electromagnetic radiation offers a promising diagnostic instrument. The underlying concept is the observation of the resonant response (when the object under study is exposed to a photon flux) occurring in the intensity of scattered photons, whose wavelengths turn out to be multiples of the linear dimensions of the microobject. The traditionally used technique is actually a version of X-ray structural analysis based on the use of a bremsstrahlung photon beam generated by a beam of accelerated electrons hitting a special radiator target. The typical disadvantage of bremsstrahlung—a wide radiation spectrum—can be compensated by additional monochromatization of the photon beam (e.g., by the well-known Bragg procedure on single crystals).

Below, we discuss one of the trends in radiation diagnostics associated with the shift of the "electron beam $\longrightarrow$ radiation" mechanism directly into the studied substance. The structural properties of the substance, which is both the bremsstrahlung radiator and the object under study in this scheme, are uniquely displayed in the radiation characteristics. This scheme noticeably extends the potential of radiation diagnostics.

2. Bremsstrahlung radiation includes both traditional bremsstrahlung (BS) on the nuclei of target atoms and polarization bremsstrahlung (PBS) on the electrons of target atoms [1, 2]. Both processes may be accompanied by coherent phenomena that are directly associated with structural features of the target material. If the wavelength of the radiated photon becomes comparable with the characteristic atomic distances in the target material (as observed in the X-ray range), the radiation process covers several bremsstrahlung centers. This stimulates coherent generation of additional in-phase photons with the same wavelength. As a result, the radiation will contain maxima with amplitudes and wavelengths that sharply depend on the local concentration of the substance and its spatial distribution, i.e., on the structure of the radiator material. All the aforesaid forms a basis for structural diagnosis of nanoobjects.

3. Note first that the total flux of generated photons and the relative contributions from BS and PBS strongly depend on the radiation angle. For fast charged particles, BS dominates at small angles, while PBS remains significant at large angles, including the backward hemisphere [2]. Consequently, observation of the radiation at different angles may yield information on both the nuclear and electron distributions in the substance.

Note also that, provided that it is possible to vary the electron beam energy, it is also possible to obtain information about the parameters of the transverse and longitudinal distributions of the substance. This is because the transverse and longitudinal characteristics of bremsstrahlung depend differently on the energy of incident electrons. The point is that the process of radiating a photon by an accelerated electron takes place over a certain length (called the coherent radiation length L_{coh}) where the generated photon and the generating electron are being spatially separated. All the bremsstrahlung centers covered by this length make a coherent (in-phase) contribution to the radiation at a given wavelength (see, e.g. [3, 4]). The coherent length is the largest when radiation occurs forward along the electron velocity; for photons with a wavelength λ, it

reaches $L_{coh} = 2\lambda\gamma^2$, where $\gamma = 1/\sqrt{1 - v^2/c^2}$ is the relativistic Lorentz factor for the radiating electron propagating at a velocity v (strong dependence on the electron energy is also observed for radiation making small angles with the electron velocity). The effective range of the transverse electron–medium interaction increases in proportion to the relativistic factor γ (see below). All these points support the statement discussed above.

The method under discussion has another important feature. Unlike conventional X-ray structural analysis with monochromatization of photons, experiments by the direct electron $\longrightarrow$ radiation mechanism do not require intense beams of accelerated electrons. On the contrary, it is more reasonable to use rather weak accelerated currents (tens–hundreds of nA), which is quite enough to obtain statistics. In this case, the radiation background sharply decreases as well, which appreciably facilitates diagnosis. Accelerators with a high duty factor [5] operating in the close-to-continuous mode are particularly promising for this purpose.

It should be noted that the special features of radiation produced by relativistic particles in substances have been extensively studied at many research centers in Russia and abroad, including the MSU SINP. However, direct studies of nanoobjects (molecular ions, fullerenes, nanotubes, fullerites, etc.) are only beginning (note, for example, [6–8]).

4. Let us confirm the above by analytical evaluations related to the detection of a nanoobject. In doing this, we restrict ourselves to the major relationships explaining the most characteristic details of the processes in question. Let us first consider the radiation of relativistic electrons slowed down by the electrons of the substance (PBS). Following the traditional procedure, where PBS is represented as scattering of the fast charge field by the target electrons [9–11], we take the spectral angular density of the radiation energy in the form

$$\frac{dW_\omega}{d\Omega} = \frac{e^6}{8\pi^3 m^2 c^3 v^2} F_{\text{eff}}, \qquad (1)$$

where W_ω is the spectral density of the radiation with a frequency ω emitted into a solid angle $d\Omega$. The factor

$$F_{\text{eff}} = \frac{v^2}{e^2}\left\langle \left| \sum_{s=1}^{Z_0} [\mathbf{n}'\mathbf{E}_\omega(\mathbf{r}_s)] \exp(-i\mathbf{q}_\omega \mathbf{r}_s) \right|^2 \right\rangle, \qquad (2)$$

where Z_0 is the number of electrons in the object, determines the total contribution from all its electrons with their position in space determined by radius $\mathbf{r}_s$. Vector $\mathbf{E}_\omega$ is the spectral amplitude of the field of a fast electron propagating at a velocity $\mathbf{v}$. Here, the field of a fast electron is represented as a virtual-wave packet [11]. The spectral amplitude of a virtual wave (only the transverse field component axially symmetrical about the electron trajectory is taken into account because the longitudinal component of the field is appreciably smaller) with a frequency ω and a wave vector $\mathbf{k} = \mathbf{v}\omega/v^2$ at a distance b from the electron trajectory is

$$E_\omega = \frac{e}{\pi b v} \zeta K_1(\zeta),$$

where $\zeta = \omega b/\gamma v$ and K_1 is the Macdonald function; in reality, $\zeta K_1(\zeta) \sim 1$ for $\zeta \le 1$ and drastically decreases when $\zeta \ge 1$. Therefore, the relation

$$\frac{\omega b}{\gamma v} \simeq 1 \qquad (3)$$

largely governs the parameters of the PBS process in question.[1] For example, the transverse action of the electron field turns out to spread at the range on the order of

$$R_\omega \simeq \frac{\gamma v}{\omega}. \qquad (4)$$

Relation (4) also makes it possible to find the limiting radiation frequency at a given size of the interaction space.

Next, the vector $\mathbf{q} = \mathbf{k}' - \mathbf{k}$, where $\mathbf{k}'$ is the wave vector of a real photon (so that $k' = \omega/c$) radiated in the direction of unit vector $\mathbf{n}'$. The pointed brackets $\langle\,\rangle$ denote averaging over possible positions of all electrons in the nanoobject.

Factor (2) includes coherent (proportional to Z_0^2) and incoherent (proportional to Z_0) contributions from the target electrons to the total radiation, which are described by the pair and the quadratic terms in the sum in (2), respectively. Since $Z_0 \gg 1$ in practically any nanoobject, the incoherent contribution is hereafter ignored.

As a result, all we need in order to make estimates is the following relation for the coherent radiation intensity

$$F_{\text{eff}} = \left(\int_{(\infty)} \frac{x \sin(q_x x)\cos(q_z z)}{x^2 + y^2} \zeta K_1(\zeta) \rho(\mathbf{r}) d\mathbf{r} \right)^2 \cos^2\psi, \qquad (5)$$

where $\rho(\mathbf{r})$ is the electron density of the object. Here, the rectangular coordinate system $\mathbf{r} = (x, y, z)$ is used and $d\mathbf{r} = dxdydz$. The z axis is directed along velocity v and runs through the center of the object, and radiation

[1] Actually, the described procedure corresponds to the motion of a charge in a vacuum. In a dense target, the charge field is subject to the material screening effect. To validate the use of this approach, we restrict our consideration to the case of weakly relativistic electrons, when their relativistic factor γ and the range of the radiation frequencies ω meet the condition $\omega^2 > \gamma^2\omega_0^2$ (ω_0 is the plasma frequency of the target material; $\hbar\omega_0 \simeq$ 30–50 eV) and the screening effect of the target material is not large.

vector $\mathbf{n}'$ lies in the (x, z) plane and makes an angle ψ with the z axis. Then, $q_x = \omega \sin\Psi/c$, $q_y = 0$, and $q_z = -\omega(1/\beta - \cos\Psi)/c$, where $\beta = v/c$.

As follows from (4) and (5), there exist optimum conditions under which electrons of an object with given spatial dimensions make the maximum coherent contribution to the total PBS yield. In particular, the longitudinal and transverse dimensions of the object and the radiation frequency should meet the requirement that the waves scattered by individual electrons should not quench each other. The coherent radiation is generated by the target electrons actually covered by the field of the fast electron. Therefore, there are two characteristic lengths that dictate the volume within which the waves resulting from the scattering of the initial field by the target electrons make an in-phase contribution to the PBS. These are the so-called longitudinal coherent length $L_{\|} \sim \pi/|q_3|$ (mentioned above in item 3) and the transverse coherent length $L_{\perp} \sim \pi/q_1$. The effect will be the largest if the length $L_{\perp}$, the transverse dimensions of the object, and the radiation frequency meet condition (4).

5. The same method using virtual photons also helps to describe traditional bremsstrahlung (BS) (by the way, application of this method to BS is quite an old technique [12]) and helps carry out comparative analysis. Following [9], we can treat the classical BS of a fast charge on a target nucleus as the scattering (in the intrinsic charge-connected reference system K', where the latter has zero translational velocity and the velocity of the nucleus is $-\mathbf{v}$) of the electromagnetic field of the nucleus. Thus, the description of BS in the K' system is reduced to the "inversion" of the formulas for PBS.

However, in reality, one should take the scattering of the total field of all charges of the nanoobject into account, including not only its nuclei but also its electrons. As a result, the effect of mutual screening should lead to a strong suppression of the BS intensity in the low-frequency region (see also [9]). It is only beginning from frequencies at which the radiation wavelength becomes smaller than the average distance between the particles of the nanoobject that BS (though only slightly coherent) may arise.

Back in the laboratory coordinate system K, two effects are worth noting: the electron screening of the field of the nucleus and the narrowing of the BS cone. This narrowing is described by the formula

$$\sin\psi = \frac{\sin\psi'}{\gamma(1 + v\cos\psi'/c)}, \qquad (6)$$

where ψ and ψ' are the radiation angles in the K and K' systems, respectively. If BS is generated by relativistic electrons, the radiation region that embraces the entire forward hemisphere in the K' system is narrowed to a cone with an opening angle of $\psi \sim 1/\gamma$. Note that the coherent BS intensity is the smallest at this angle (see (6)). Yet, the considerations above confirm the ability to obtain various kinds of information on the structure of nanoobjects by measuring the X-ray radiation emitted at small and large angles.

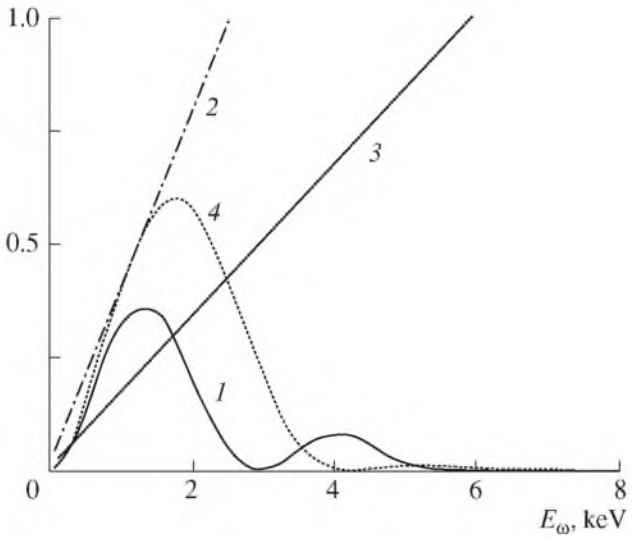

Fig. 1. Parameters of the PBS of fast electrons with the relativistic factor $\gamma = 10$ on the spherical fullerene of diameter $d = 0.7$ nm at the radiation angle $\psi = \pi/4$ vs. photon energy: factor F_{eff} for (*1*) one-layer fullerene and (*4*) fullerene with internal atoms and (*2*) longitudinal and (*3*) transverse reduced phases $q_1 d/2\pi$ and $q_3 d/2\pi$.

6. Let us illustrate the above by a particular numerical evaluation of the PBS from an interesting nanoobject, viz., fullerene, where the PBS of relativistic electrons is known to feature additional interference effects. As is known, the fullerene molecule is a nanoobject consisting of tens to hundreds of atoms of one or several sorts arranged into one or several thin layers [13]. The size of one-layer fullerenes is on the order of 1 nm. For example, the most abundant spherical fullerene C_{60} is 0.7 nm in diameter.

The results of numerical calculation of the factor F_{eff} for PBS from spherical fullerene C_{60} of diameter $d = 0.7$ nm are depicted in Fig. 1, which shows the dependence of F_{eff} (in relative units per electron of the nanoobject) on the energy of radiated photons in two model cases. Curve *1* is for a one-layer thin-wall fullerene, and curve *4* is for a similar fullerene with an inner inclusion of atoms of the same sort.

Since the observable PBS results from interference summation of radiation signals from all atoms of the object, the following characteristic pattern can be traced. In the low-frequency region, where the radiation wavelength λ is larger than the size of the object (these values are compared at the photon energy $E_\omega \sim 2$ keV), all the fullerene electrons radiate practically "in unison" with each other, thus giving rise to a sharp and

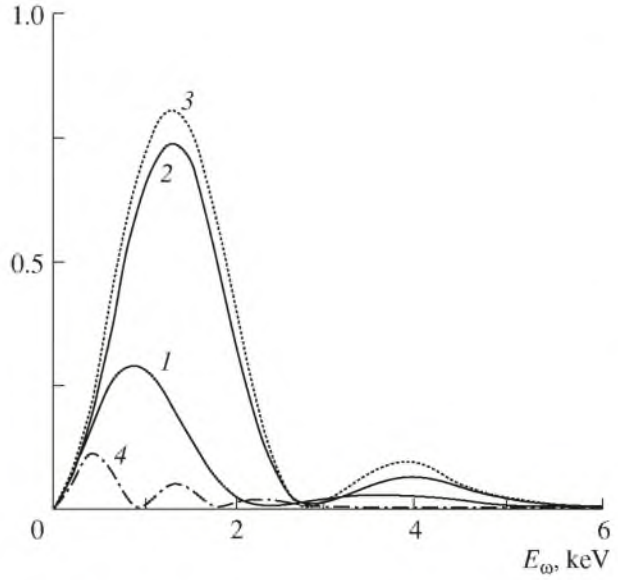

Fig. 2. Factor F_{eff} in the PBS of fast electrons on the spherical one-layer C_{60} fullerene of diameter $d = 0.7$ nm vs. photon energy. Curves *1*, *2*, and *3* are for radiation angle $\psi = \pi/4$ and $\gamma = 10$, 50, and 100 respectively; curve *4* is for $\psi = 3\pi/4$ and $\gamma = 10$.

coherent PBS peak. At higher photon energies (and, accordingly, at smaller wavelengths), electrons at opposite sides of the fullerene emit PBS radiation in mutually quenching phases, and the sum PBS is only low. The minimum of F_{eff} is observed at $q_3 d_{\text{eff}} \simeq \pi$, where d_{eff} is the effective distance between the centers of the electron distributions at the front and rear parts of the fullerene ($d_{\text{eff}} < d$). The F_{eff} minimum is at an energy of approximately 3 keV for one-layer thin-wall fullerene and at about 4 keV for the fullerene with inner atoms. One more effect manifests itself in the latter case: fullerene electrons are on the average closer to the path of the incident particle and its field effect is accordingly stronger, which shows itself in a higher signal amplitude in curve *4*. Owing to the phase interplay (phase variation is indicated by lines *2* and *3*), the PBS intensity oscillates and gradually decays.

Figure 2 plots the factor F_{eff} for the one-layer C_{60} fullerene versus the energy of photons radiated at the angle $\psi = \pi/4$ for different relativistic factors of fast electrons (curves *1*, *2*, and *3*) and at $\psi = 3\pi/4$ (curve *4*). The amplitude saturation of the coherent peak of F_{eff} with an increase in relativistic factor γ (curves *1–3*) is in line with the ideas under discussion on the character of the relativistic electron radiation. Specifically, the longitudinal coherence length $L_\parallel$ for radiation at 1 keV becomes comparable with the diameter of the fullerene, even when the relativistic factor is close to ten. An increase in the relativistic factor may lead to a noticeable growth of the peak of $L_\parallel$ (but not of $L_\perp$, which does not show a dependence of this type) only in more complicated systems, e.g., in a fullerene chain, where the growing coherent length accommodates an increasingly large number of neighboring objects. A comparison of curves *2* and *4* also confirms this. At the radiation angle $\psi = 3\pi/4$, q_3 noticeably increases and $L_\parallel$ decreases. Therefore, the amplitude of the coherent signal sharply drops and the oscillation period decreases.

Thus, although the examples considered were only of a model character, the numerical data confirm the stated qualitative assumptions about the potentiality of coherent radiation diagnostics of nanoobjects. It should be stressed that the amplitude of coherent radiation generated by relativistic electrons scattered from a nanoobject is proportional to the number of its electrons squared. For example, the intensity of PBS from the C_{60} fullerene is 60^2 times higher than that from a single carbon atom. Further research efforts are necessary in order to produce a detailed structural study of materials containing nanoobjects, an analysis of more complicated nanocomplexes, and other details of PBS.

7. In conclusion, it is worth noting that theoretical and experimental studies in this direction are now planned at the 70-MeV race-track microtron recently put into operation at the MSU SINP. This new-generation accelerator provides for high-quality electron beams with energies from 6 to 70 MeV [14], which open a wide range of possibilities for studying different radiation mechanisms and their applications (see also [15]).

ACKNOWLEDGMENTS

This study was supported by grant of the President of the Russian Federation for Support of Leading Scientific Schools, no. NSh-5365.2006.2, and by the Russian Foundation for Basic Research, projects nos. 05-02-17648 and 06-02-16714.

REFERENCES

1. M. L. Ter-Mikaelian, *High Energy Electromagnetic Processes in Condensed Media* (Wiley, New York, 1972).
2. M. Amus'ia, V. Buimistrov, B. Zon, et al., *Polarization Bremsstrahlung of Particles and Atoms* (Plenum, New York, 1992).
3. V. A. Bazylev and N. K. Zhevago, Usp. Fiz. Nauk **137** (4), 605 (1982).
4. B. M. Bolotovskii, Tr. Fiz. Inst. Akad. Nauk SSSR **140**, 94 (1984).
5. J. E. E. Baglin, A. J. Bureau, B. C. Cook, et al., in *Proceedings of the 5th Particle Accelerator Conference: Accelerator Engineering and Technology, San Francisco, California, 1973*, IEEE Trans. Nucl. Sci. **20**, 932 (1973).

6. V. K. Grishin, Nucl. Instrum. Methods Phys. Res. B **227** (1–2), 82 (2005).
7. V. K. Grishin, in *Proceedings of the Particle Accelerator Conference PAC-2005, Knoxville, 2005*; http://snsapp1.sns.ornl.gov/pac05, RPAP018.
8. N. Nasonov, V. Kaplin, S. Uglov, et al., Nucl. Instrum. Methods Phys. Res. B **227** (1–2), 41 (2005).
9. A. I. Akhiezer, and I. B. Berestetskii, *Quantum Electrodynamics* (Nauka, Moscow, 1969,), par. 26 [in Russian].
10. L. D. Landau and E. M. Lifshitz, *Field Theory* (Fizmatgiz, Moscow, 1960), par. 80 [in Russian].
11. W. K. H. Panofsky and M. Phillips, *Classical Electricity and Magnetism* (Addison–Wesley, Reading, 1962), par. 18.5.
12. E. Fermi, Z. Phys. **29**, 315 (1924).
13. A. S. Fialkov, *Carbon Compounds and Carbon-Based Composites* (Aspekt, Moscow, 1997) [in Russian].
14. V. I. Shvedunov, A. N. Ermakov, I. V. Gribov, et al., Nucl. Instrum. Methods Phys. Res. A **550**, 39 (2005).
15. A. N. Baldin, I. E. Vnukov, V. K. Grishin, et al., in *Proceedings of the 36th International Conference on Physics of Interaction of Charged Particles with Crystals, Moscow, 2005*, p. 80.